The flow around stationary and elastically-mounted circular cylinders in tandem and staggered arrangements

Martin Griffith, David Lo Jacono, John Sheridan, Justin S. Leontini

The Flow Around Stationary and Elastically-Mounted Circular Cylinders in Tandem and Staggered Arrangements

M. D. Griffith[1], D. Lo Jacono[3], J. Sheridan[2] and J. Leontini[1]

[1]Swinburne University of Technology, Hawthorn, Victoria, 3122, Australia

[2]Fluids Laboratory for Aeronautical and Industrial Research (FLAIR), Department of Mechanical & Aerospace Engineering, Monash University, Melbourne, Victoria, 3800, Australia

[3]Université de Toulouse; INP; IMFT (Institut de Mécanique des Fluides de Toulouse), Allée Camille Soula, F-31400 Toulouse, France; CNRS; IMFT; F-31400 Toulouse, France

Abstract

A numerical study is presented of the flow around two circular cylinders in tandem and staggered arrangements in a freestream, examining the fluid forces and vortex-shedding behaviour, as well as the oscillation of both cylinders when allowed to move and vibrate in response to the flow. The streamwise distance between the cylinder centres is 1.5 diameters, while the cross-stream offset is varied from 0.0 to 5.0. The Reynolds number, based on cylinder diameter, D, and freestream velocity, U, is 200. Reduced velocity, $U^* = \frac{U}{f_N D}$, where f_N is the spring natural frequency, is varied from 0.0 to 14.0. Results are obtained using a sharp-interface immersed boundary finite-difference method. For the stationary cylinders a range of behaviours are observed over the cylinder offset range, including a difference in primary vortex-shedding frequency when the crossstream offset is greater than $1.5D$. For the elastic-mounting, in contrast to existing results in the literature, three modes of vortex-shedding and oscillation are observed over the U^* range for the tandem arrangement. These modes are distinct in the phase difference between the front and rear cylinder oscillation, as well as the number of vortices shed from each cylinder.

Introduction

The vibration of an elastically-mounted circular cylinder in a flow is a canonical problem in fluid-structure interaction and a large volume of literature exists on the subject [4, 8, 6, 10]. Large amplitude oscillations occur when the vortex-shedding frequency matches with the cylinder oscillation frequency. This lock-in regime occurs over a range of natural frequencies for the elastic cylinder mounting [11]. The behaviour of the system is useful as a fundamental case for more irregular or complex geometries. For example, in applications where the potential for high-amplitude oscillation is critical, such as in the design of oil drilling risers and other marine structures. Similarly, high-amplitude oscillation may be beneficial for the extraction of energy from VIV for power generation.

One such geometrical complexity to be considered is the presence of another, or several, cylinders in the vicinity of the single, isolated cylinder. When two stationary cylinders in cross-flow are placed close enough together, their wakes begin to interfere. Figure 1 depicts the problem setup. The streamwise distance between the centres of the cylinders is defined as L and the cross-stream distance as T. For two cylinders, there are three arrangements possible: tandem, side-by-side and staggered. Tandem cylinders are arranged inline to the flow ($L \geq D$, $T = 0.0$). Side-by-side cylinders are side-by-side with respect to the oncoming flow ($L = 0.0$, $T \geq D$). For staggered cylinders, there is both a streamwise and cross-stream offset ($L > 0$, $T > 0$, $\sqrt{L^2 + T^2} \geq D$). Staggered cylinders arrangements are also often defined in terms of a pitch ratio, P/D, where P is the distance between the cylinders, and an incidence angle, α. For stationary cylinders, a range of regime definitions have been proposed, depending on the proximity and interactions of the wakes of each cylinder [7]. Tong, Cheng and Zhao [9] defined four flow classifications: S-I, where only one vortex street exists with vortices shed from the downstream cylinder; S-II, again only one vortex street, but vortices shed from both cylinders; T-I, two vortex streets exist but with strong interactions; and T-II, two vortex streets but with weak interactions. For the S-I and S-II classifications, one cylinder sits in the wake of the other and, if the downstream cylinder is close enough, no vortices are able to shed from the upstream.

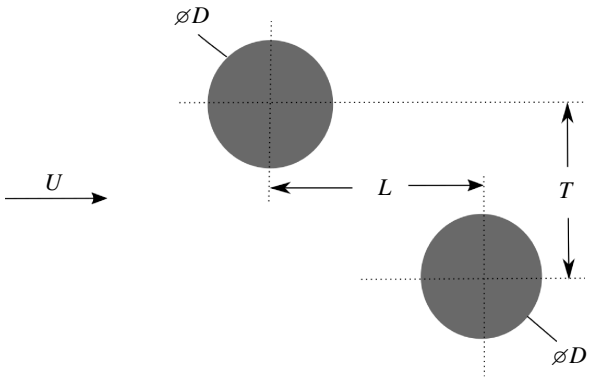

Figure 1: A sketch of the setup.

For elastically-mounted cylinders, Borazjani and Sotiropoulos [2] investigated the tandem cylinder arrangement, with an in-line offset of $L = 1.5D$. The cylinders were found to oscillate at greater amplitudes than a single, isolated cylinder and also to experience greater lift force. Other studies have examined similar problem configurations: with two rigidly-coupled cylinders in tandem and side-by-side arrangement [12]; with side-by-side cylinders with two degrees of freedom [3]; and with tandem cylinders with the upstream cylinder stationary and the downstream oscillating, [1].

The current study examines the tandem arrangement, with $L = 1.5$, as a starting point, over a range of reduced velocities. The work is then extended to the staggered arrangement by increasing the cross-stream offset, T.

Problem Definition

The geometry has been defined in figure 1. The two cylinders are aligned such that their centres are a distance L/D apart in the streamwise direction and T/D apart in the cross-stream direc-

tion. The cylinders are arranged equidistant around the origin. In the results presented here, the upstream cylinder is positioned at $y \geq 0$ and the downstream cylinder at $y \leq 0$. The Reynolds number is defined as

$$Re = \frac{UD}{\nu}, \tag{1}$$

where U is the fluid freestream velocity, D the cylinder diameter and ν the kinematic viscosity. The ratio of the mass of each cylinder to the mass of the equivalent volume of fluid is defined as $m^* = 2.546$, as used in Borazjani and Sotiropoulos [2] in their of study tandem vibrating cylinders. Each cylinder is elastically-mounted; the natural frequency of the springs is given as $f_N = \sqrt{k/M}/2\pi$, where k is the spring stiffness and M is the mass of the cylinder. A non-dimensional reduced velocity is defined such that $U^* = U/Df_N$. There is no damping added to the system. The y-position of a cylinder is defined as Y and the oscillation of each cylinder is defined by the equation:

$$M\left(\ddot{Y} + (2\pi f_N)^2 Y\right) = F_y, \tag{2}$$

where $\ddot{Y}$ is the acceleration of the cylinder perpendicular to the freestream and F_y is the lift force on the cylinder. The position of the cylinders can be described as:

$$Y_1 = \overline{Y}_1 + Y_1' + T/2, \tag{3}$$
$$Y_2 = \overline{Y}_2 + Y_2' - T/2, \tag{4}$$

where $\overline{Y}$ is the mean position with respect to the cylinder starting point, Y' is the oscillatory component of the cylinder motion and the subscripts 1 and 2 denote the front and rear cylinders, respectively.

Method

Simulations were carried out using a sharp-interface immersed boundary method to represent the cylinders on an underlying Cartesian grid, on which the flow is simulated by solving the incompressible Navier-Stokes equations using a finite-difference scheme [5]. The vibration of each cylinder is found by solving equation 2 using a Newmark-β method. The underlying Cartesian grid was designed with a regular grid spacing around the origin, over a box-region measuring $4D$ in each direction. Grid spacings were then increased linearly to the domain boundaries. The inlet and lateral domain boundaries were located $15D$ from the origin, while the outlet boundary was located $40D$ downstream. Twice as many grid points were used in the streamwise direction than in the transverse direction; the number of grid points in each direction is restricted to the powers of 2, thereby leading to a grid size of $2^{N+1} \times 2^N$, where N is a whole number. We denote each grid as MN, such that $M10$ corresponds to a grid size of 2048×1024 nodes.

A test of the sensitivity of the results to grid resolution was carried out. For the tandem cylinder arrangement of offset $T = 0.0$, results were obtained over the U^* range for grids $M8$, $M9$, $M10$ and $M11$. For the grid $M9$, the results returned for A^*_{MAX} are within 1% of the result returned by the higher resolution M10 grid, while the root-mean-square value of the lift coefficient is within 2%. For all the results presented here for $T \leq 3.5$, grid M9 was used. For the upper range of cylinder offset, $T > 3.5$, the box-region of regular grid spacing around the origin was increased to $8D$ in the y-direction to encompass the wider wake width and cylinder vibration that these cylinder arrangements produce. For this grid the number of total grid points in the y-direction was doubled for the $M9$ grid, maintaining the same transverse domain boundary distance, but using the extra grid points to increase the size of the box-region of regular grid spacing. Simulations run for values of $T < 3.5$ using both grids showed negligible differences in oscillation amplitude and mean force coefficient.

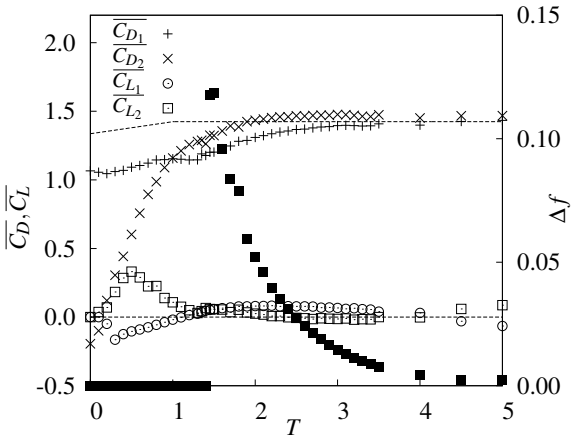

Figure 2: For stationary cylinders and $L = 1.5$, the variation with cross-stream offset, T, of the mean values of the drag and lift coefficients for the front and rear cylinders, denoted by subscripts 1 and 2, respectively. On the right axis, in solid squares (■), the variation of the difference in the primary frequency of the oscillation of the two cylinders. The dotted lines refer to the mean drag and lift coefficients returned by a single cylinder, with the drag coefficient corrected by a ratio of the squares of the blockage ratios of the single and the double cylinder simulations, assuming a side-by-side arrangement.

Results

Stationary cylinders

The first set of results for stationary cylinders represents a limiting case of equation 2 where $U^* = 0$, producing no flow-induced vibration. For inline cylinders, the current results are consistent with results presented in the literature for mean drag coefficient [9]. Introducing a cross-stream offset, figure 2 plots the variation of the mean values of the lift and drag coefficients for both cylinders. For the inline cylinders, most of the drag is experienced by the front cylinder; the rear cylinder experiences a negative mean drag. The negative mean drag on the rear cylinder only occurs for offsets $T < 0.2$. The drag increases almost linearly up to offset $T = 1.0$, from which point it exceeds the drag on the front cylinder. The mean lift force is zero for both cylinders for the symmetric tandem configuration. With increasing offset, the mean lift becomes positive for the rear cylinder and negative for the front, indicating a mean force on the cylinders away from the centreline . Around $T = 1.2$, the drag on the front cylinder becomes positive again. Further increasing the offset from this value, the two values of $\overline{C_L}$ slowly converge.

Beyond an offset of $T = 1.5$, a difference in the primary frequency of vortex-shedding, Δf, appears (calculated from frequency analysis of the signal for the coefficient of lift) and is associated with a loss of order in the vortex shedding. The primary frequency difference decreases with increasing offset, manifesting as a beating (of increasing period) in the lift signal of each cylinder. For $T > 2.3$, the vortex-shedding is ordered, with the values for $\overline{C_D}$ and Δf converging to their values for the single cylinder. Note, that the value of the drag coefficient for the single cylinder has been corrected in an attempt to account for the difference in effective blockage ratio between one or two cylinders presenting fully to the freestream flow. Although the cylinders are at different streamwise positions and that strictly

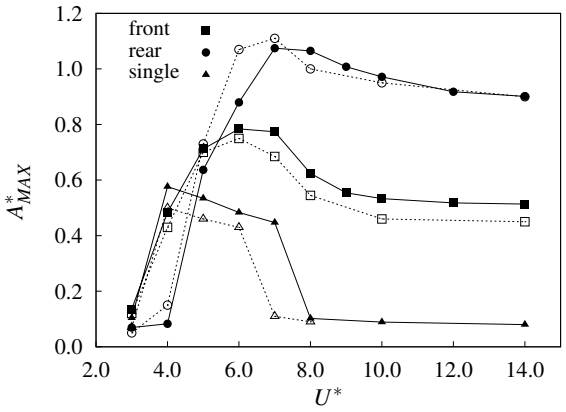

Figure 3: For $T = 0.0$ and $L = 1.5$, the variation with U^* of the maximum displacement of the each cylinder. Solid symbols represent results from the current study, while hollow ones are from Borazjani and Sotiropoulos [2].

the blockage ratio for the two cylinder simulations is not different to that of a single cylinder, the actual effect on the cylinders will depend on the nature of the flow in the gap between the cylinders, which in turn depends on the fluid dynamics near the cylinders. From figure 2, the correction of the mean drag coefficient for the single cylinder empirically seems appropriate given the convergence of the drag coefficients as $T \to 5$. Although only tests for offsets of $T > 5.0$ could confirm this.

Vibrating Cylinders, $T = 0.0$

Borazjani and Sotiropoulos [2] present results for $T = 0.0$ and $L = 1.5$ and for the reduced velocity range $3 \leq U^* \leq 14$. The same parameter space has been simulated using our method, giving the results in figure 3, showing maximum displacement, A^*_{MAX}, for each cylinder for comparison. We calculate A^*_{MAX} as the mean of the greatest 10% of local peaks of Y. Across the three parameters presented there are differences with the results from the literature [2]. For the single isolated cylinder, the values of A^*_{MAX} for the range $4 \leq U^* \leq 7$, for the current study are greater than those reported previously. For the tandem arrangement, the oscillation amplitude of the front cylinder is greater, while that of the rear cylinder is reduced slightly for $5 \leq U^* \leq 7$. Similarly for the lift and drag, some variation in the results can be seen (not shown here).

The comparison shows the variations with U^* of oscillation amplitude, A^*_{MAX}, and the root-mean-square coefficients of lift and drag (not plotted) are similar between the two studies, but there are significant variations between the two studies for some values of U^*. We put these differences down principally to the different domain sizes used in each study, as well as differences in grid resolution. Borazjani and Sotiropoulos [2] used an inlet length and lateral clearance of $8D$ and an outlet length of $24D$. Therefore, there is a significant difference in blockage ratio between the two studies: for a single cylinder, 6.25% against 3.33% for the current study. In an attempt to account for this difference, we ran the results for a single, isolated cylinder again, but with a domain size reduced to that used in [2]. This produced only marginal differences in the returned results for A^*_{MAX}. There is also a significant difference in timestep used between the two studies; $\delta t = 0.02$ in [2] and $\delta t = 0.004$ in the current. This difference is mostly due to the higher grid resolution used in the current study. To examine the effect of timestep, we have also run both grid domain sizes using timesteps of $\delta t = 0.004$ and 0.002, to examine any sensitivity to temporal resolution. We found no significant effect resulting from this change in timestep.

For zero cross-stream offset, $T = 0.0$, Borazjani and Sotiropoulos [2] defined two flow states which we summarize here. State 1 refers to those cases where the front cylinder oscillated more than the rear, for $U^* \leq 4.0$, and state 2, where the rear cylinder oscillated more, for $U^* \geq 7.0$. They classed the cases in between these two ranges as critical cases in the transition between the two states. Using the vortex-shedding pattern classification of Williams and Roshko [11], state 1 consists of a $2S$ vortex-shedding pattern, where a single vortex of each sign is shed from the rear cylinder, with the rear cylinder enveloped by shear layers beginning at the front cylinder. State 2 consists of a $2P$ vortex-shedding pattern, with vortices of each sign shed from both cylinders with complex vortex interaction and merging in the near-wake. The critical case for $U^* = 5.0$ shows similarity to state 2, but does not show a $2P$ ordering, with complex interactions resulting from fast moving vortex pairs merging with earlier-shed vortices, producing a less ordered wake.

We propose that the two states described in the literature [2] are better described as vortex-shedding modes, and that the critical case ($U^* = 5.0$ and 6.0) is in fact its own distinct vortex-shedding mode, rather than a transition case. Mode 1 refers to those cases where the rear cylinder oscillation is small, $U^* \leq 4.0$, and is synonymous with the state 1. Mode 2 is present for $U^* = 5.0$ and 6.0, while mode 3, (synonymous with state 2) exhibits large rear cylinder oscillation and is present for $U^* \geq 7.0$. Plots of vorticity contours throughout the oscillation for representative cases of each of the three modes are shown in figure 4. For mode 1, shown for $U^* = 4.0$, the rear cylinder sits in the wake of the front throughout the oscillation cycle. The oscillation of the rear cylinder is comparatively small and lags the oscillation of the front cylinder by $\gamma = 4\pi/5$, or 0.4 of an oscillation cycle. Vorticity that forms on the front cylinder merges with vorticity of the same sign on the rear cylinder. Vortices are shed only from the rear cylinder. One vortex of each sign is shed each cycle, forming a regular vortex street. Given the vortices shed from the rear cylinder, we denote this mode as $2S_R$. The mode exists for cases of $U^* = 3.0$ and $U^* = 4.0$, with simulations requiring long run times ($750U^*$) to reach a statistically-converged solution.

Mode 2 exists for $U^* = 5.0$ and 6.0. For these cases, the rear cylinder oscillates more than it does for mode 1, coming out fully from behind the front cylinder. The cylinders oscillate out of phase, $\gamma = \pi$. In contrast to mode 1, vortices do not form on the rear cylinder, instead only a small amount of vorticity is deposited in a trail. Instead a vortex pair forms in the periodically larger space now available between the cylinders. As this pair forms it is cut off by the rear cylinder, its orientation rolling before meeting freestream fluid and convecting at high velocity downstream. The vortex pairs overtake earlier pairs, merge and form an irregular vortex street. Because of the two vortex pairs formed each cycle, which mostly form on the front cylinder, we denote this mode $2P_F$,

Mode 3 exists for $U^* \geq 7.0$ and is characterised by large oscillation of the rear cylinder, with the oscillation of the rear cylinder lagging the front cylinder by $\gamma \approx \pi/2$. Similar to mode 2, the rear cylinder traverses the wake of the front, but instead of a vortex pair forming in the gap, the rear cylinder effectively cuts through the shear layers of the front cylinder (the second to third images of figure 4). In a complex interaction, negative and positive vorticity from the front cylinder is subsumed by the vortex formation on the rear cylinder each half cycle. Each cycle, this vortex mingling creates two pairs of unequal strength vortices. To account for the complex formation of these vortex pairs, the mode is denoted as a $2P$. These three vortex-shedding

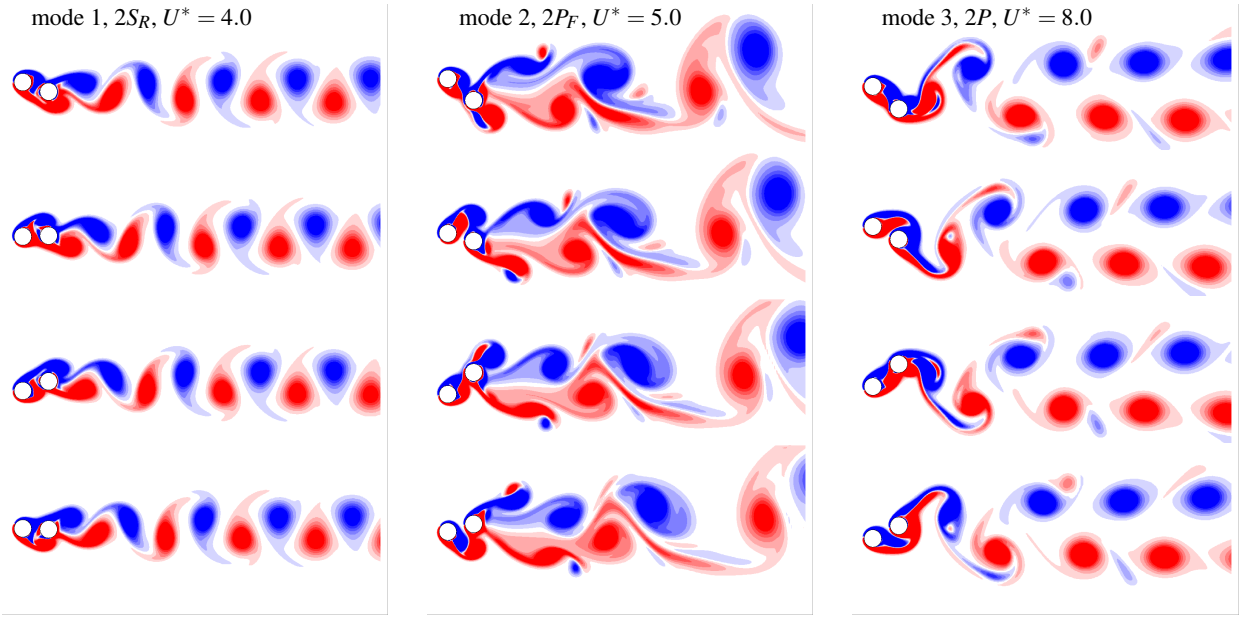

Figure 4: For the tandem cylinder arrangement ($T = 0$), vorticity contours for three cases, $U^* = 4.0$, 5.0 and 8.0, describing the three vortex-shedding modes, $2S_R$, $2P_F$ and $2P$. Each series of images depicts an entire oscillation cycle, beginning with the front cylinder at its maximum displacement. Contours vary in the range $-1 \leq \omega_z \leq 1$.

modes cover the $T = 0.0$ parameter space.

Conclusions

Results for the flow around tandem and staggered cylinder pair configurations for stationary cylinders have been presented, exhibiting a variation with transverse offset of the the lift and drag coefficients on the cylinders and of the difference of the primary frequency of vortex-shedding. The results are consistent with published results in the literature. The flow around and vibration of elastically-mounted cylinders for the tandem arrangement has also been presented, with three distinct modes of oscillation and vortex-shedding identified across the range of U^* and characterized by differences in phase lag between the cylinder oscillations and in the number of vortices shed from each cylinder. Future work will extend into the cross-stream offset parameter space for the elastically-mounted cylinders.

Acknowledgements

This work was financially supported by the Australian Research Council (ARC) through Discovery Projects grant DP150103177. Computational resources provided by the National Computational Infrastructure (NCI) under project IZ4 through the National Computational Infrastructure Merit Allocation Scheme (NCMAS), and by Swinburne University of Technology's Centre for Astrophysics and Supercomputing.

References

[1] Assi, G. R. S., Bearman, P. W., Meneghini, J. R., On the wake-induced vibration of tandem circular cylinders: the vortex interaction excitation mechanism, *J. Fluid Mech.*, 2010, **661**, 365–401.

[2] Borazjani, I., Sotiropoulos, F., Vortex-induced vibrations of two cylinders in tandem arrangement in the proximity-wake interference region, *J. Fluid Mech.*, **621**, 2009, 321–364.

[3] Huera-Huarte, F. J., Gharib, M., Flow-induced vibrations of a side-by-side arrangement of two flexible circular cylinders, *J. Fluids Struct.*, **27**, 2011, 354–366.

[4] Leontini, J. S., Thompson, M. C., Hourigan, K., The beginning of branching behaviour of vortex-induced vibration during two-dimensional flow, *J. Fluids Struct.*, **22**, 2006, 857–864.

[5] Mittal, R., Dong, H., Bozkurttas, M., Najjar, F. M., Vargas, A., von Loebbecke, A., A versatile sharp interface immersed boundary method for incompressible flows with complex boundaries, *J. Comp. Physics*, **227**, 2008 4825–4852.

[6] Singh, S. P., Mittal, S., Vortex-induced oscillations at low Reynolds numbers: Hysteresis and vortex-shedding modes, *J. Fluids Struct.*, **20**, 2005 1085–1104.

[7] Sumner, D., Two circular cylinders in cross-flow: A review, *J. Fluids Struct.*, **26 (6)**, 2010, 849–899.

[8] Thompson, M. C., Hourigan, K., Sheridan, J., Three-dimensional instabilities in the wake of a circular cylinder, *Exp. Therm. Fluid Sci.*, **12**, 1996 190–196.

[9] Tong, F., Cheng, L., Zhao, M., Numerical simulations of steady flow past two cylinders in staggered arrangements, *J. Fluid Mech.*, **765**, 2015, 114–149.

[10] Williamson, C. H. K., Govardhan, R., Vortex-induced vibrations, *Annu. Rev. Fluid Mech.*, **36**, 2004, 413–455.

[11] Williamson, C. H. K., Roshko, A., Vortex formation in the wake of an oscillating cylinder, *J. Fluids Struct.*, **2**, 1988, 355–381.

[12] Zhao, M., Flow induced vibration of two rigidly coupled circular cylinders in tandem and side-by-side arrangements at a low Reynolds number of 150, *Phys. Fluids*, **25**, 2013, 123601.